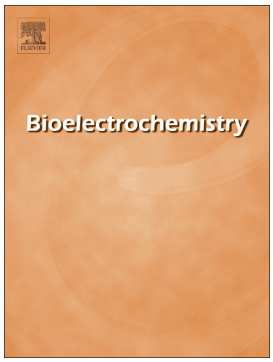

A highly sensitive electrochemical biosensor for phenol derivatives using a graphene oxide-modified tyrosinase electrode

Yue Wang, Fengge Zhai, Yasushi Hasebe, Hongmin Jia, Zhiqiang Zhang

PII: S1567-5394(17)30647-3
DOI: doi:10.1016/j.bioelechem.2018.04.003
Reference: BIOJEC 7139

To appear in: *Bioelectrochemistry*

Received date: 26 January 2018
Revised date: 4 April 2018
Accepted date: 6 April 2018

Please cite this article as: Yue Wang, Fengge Zhai, Yasushi Hasebe, Hongmin Jia, Zhiqiang Zhang , A highly sensitive electrochemical biosensor for phenol derivatives using a graphene oxide-modified tyrosinase electrode. The address for the corresponding author was captured as affiliation for all authors. Please check if appropriate. Biojec(2017), doi:10.1016/j.bioelechem.2018.04.003

A highly sensitive electrochemical biosensor for phenol derivatives using a graphene oxide-modified tyrosinase electrode

Yue Wang[1,*], Fengge Zhai[1], Yasushi Hasebe[2], Hongmin Jia[1], Zhiqiang Zhang[1,*]

[1] School of Chemical Engineering, University of Science and Technology Liaoning, 185 Qianshan Middle Road, High-tech zone, Anshan, Liaoning, 114051, China.

[2] Department of Materials Science and Engineering, Graduate School of Engineering, Saitama Institute of Technology, 1690 Fusaiji, Fukaya, Saitama 369-0293, Japan.

Corresponding author 1:

Tel.: +86 412 5929269; fax: +86 412 5929627

E-mail: wangyue@ustl.edu.cn (Yue Wang).

185 Qianshan Middle Road, High-tech zone, Anshan, Liaoning, 114051, China.

Corresponding author 2:

Tel.: +86 412 5928009; fax: +86 412 5928009

E-mail: zhangzhiqiang@ustl.edu.cn (Zhiqiang Zhang).

185 Qianshan Middle Road, High-tech zone, Anshan, Liaoning, 114051, China.

Abstract

The fabrication, characterization and analytical performance were investigated for a phenol biosensor based on the covalent bonding of tyrosinase (TYR) onto a graphene oxide (GO)-modified glassy carbon electrode (GCE) via glutaraldehyde (GA). The surface morphology of the modified electrode was studied by atomic force microscope (AFM) and field-emission scanning electron microscopy (FE-SEM). The fabricated TYR/GA/GO/GCE biosensor showed very good stability, reproducibility, sensitivity and practical usage. The catechol biosensor exhibited a wide sensing linear range from 5×10^{-8} M to 5×10^{-5} M, a lower detection limit of 3×10^{-8} M, a current maximum (I_{max}) of 65.8 μA and an apparent Michaelis constant (K_m^{app}) of 169.9 μM.

Keywords: tyrosinase, graphene oxide, covalent bonding, phenol derivatives, glassy carbon electrode

1. Introduction

Phenol derivatives are industrial chemicals widely used in the manufacturing of products. Most of them are generated artificially and are found in the wastewater of chemical plants, exhaust gases from incinerators, sidestream smoke from cigarettes, and so on.[1,2] Many phenol derivatives are very toxic, showing adverse effects on living things. High levels of phenols have detrimental effects on animal health. Prolonged oral or subcutaneous exposure causes damage to the lungs, liver, kidney and genitourinary tract.[3] Therefore, the determination of phenol derivatives is of great importance.

The phenol derivatives are detected by various methods such as calorimetry, photometry, chromatography and capillary electrophoresis.[4-7] However, these procedures usually require time-consuming as well as complicated sample pretreatment and lack satisfactory sensitivity. Electroanalysis has been developed considerably during the past decades due to its high sensitivity and rapid portable analysis. Therefore, many biosensors based on phenol oxidases have been developed to offer an attractive alternative approach to monitoring the phenol derivatives.[8-17]

Tyrosinase (TYR, polyphenol oxidase, EC 1.14.18.1) is a binuclear copper-containing metalloprotein that possesses two different catalytic activities (i.e., monophenolase activity, the ortho-hydroxylation of monophenols, and diphenolase activity, the oxidation of *o*-diphenols to *o*-quinones).[18,19] It is the well-known phenol oxidase that is widely distributed in microorganisms, plants and animals.[20,21] Enzymatically produced quinone can be electrochemically reduced back to catechol at a relatively moderate potential (ca. 0 V vs. Ag/AgCl on a carbon electrode). The signal was amplified by the recycling of catechol, and therefore, amperometric biosensors based on tyrosinase exhibit high selectivity and sensitivity with the potential for miniaturization and automation.[22]

Since Novoselov's "groundbreaking experiments regarding the two-dimensional material in 2004",[23] tremendous research efforts have been carried out toward the study and applications of graphene and graphene-based materials. Graphene oxide has

potential applications in the construction of nonenzymatic electrochemical sensors due to its advantages of good dispersion and a variety of functionalization methods.[24,25] It has a large surface area to volume ratio and good biocompatibility. GO is also an amphiphilic molecule, and its hydrophilicity makes it highly dispersible in water, whereas its hydrophobicity provides active sites for interaction with other compounds.[26] Due to the aforementioned properties, graphene oxide is a potential matrix for electrochemical biosensors.[27]

In this paper, we describe highly sensitive biosensors for phenol derivatives based on tyrosinase immobilized onto a GO-modified glassy carbon electrode (GCE). First, the GO was cast onto the GCE surface. Then, the glutaraldehyde was bonded to the GO via the –OH groups on the GO sheet. Finally, TYR was immobilized on the GA/GO-modified surface. It is important to use GO as the supporting matrix because of the –OH groups it contains, which provide the essential functional group for further covalent bonding. The immobilization of TYR was realized via self-assembly under mild conditions. Compared with other functionalized graphene composite-modified TYR biosensors, this sensor shows a comparable performance, wide linear range and high sensitivity with a rather facile fabrication protocol.

2. Experimental

2.1 Apparatus

The morphology of the prepared biosensor was evaluated using a field-emission scanning electron microscopy (FE-SEM) instrument (ΣIGMA-HD, ZEISS). The AFM images were recorded with a multimode scanning probe microscope system operated in the tapping mode using a Being Nano-instruments CSPM-5500 (Ben Yuan Ltd., Beijing, China). An FT-IR spectrum was recorded in the range of 500 to 4000 cm^{-1} on a Nicolet (is10) FT-IR spectrometer. Electrochemical measurements were performed on a CHI 750D workstation (Shanghai Chenhua, China). A conventional three-electrode system with a modified glassy carbon electrode (GCE) with a diameter of 3 mm as the working electrode, a thin Pt wire as the counter electrode and Ag/AgCl (sat. KCl) as the reference electrode was used. To compare the interfacial properties of the modified surfaces, electrochemical impedance spectroscopy (EIS) was performed by using deoxygenated 0.1 M phosphate buffer (pH = 7.0, 15 mL) containing 1 mM $Fe(CN)_6^{4-/3-}$. The applied potential was set at the formal potential of the $Fe(CN)_6^{4-/3-}$ redox reaction (i.e., 0.23 V vs. Ag/AgCl at pH = 7.0). The frequency ranged from 0.01 Hz to 10 kHz. All measurements were performed in air at room temperature (~20°C).

2.2 Reagents and Materials

Tyrosinase (TYR, polyphenol oxidase, EC 1.14.18.1; 1715 units/mg from mushrooms), glutaraldehyde (GA), cyanuric chloride (CC), 1,4-benzoquinone (BQ), ascorbic acid (AA), glyoxal solution (GX), terephthaloyl chloride (TPC) and *p*-cresol were purchased from the Sigma-Aldrich Trade Co., Ltd. and used as received. Graphene oxide (GO) was obtained from the Suzhou Tanfeng Graphene Tech Co., Ltd. Catechol, phenol, *p*-chlorophenol (*p*-CP), hydrogen peroxide (H_2O_2), uric acid (UA) and glucose were obtained from the Sinopharm Chemical Reagent Co., Ltd. A 0.1 M phosphate buffer solution (PBS, prepared by using K_2HPO_4 and KH_2PO_4) was used to prepare the electrolyte. All reagents were used without further purification. Doubly distilled water was used throughout the experiments.

2.3 Fabrication of the TYR/GA/GO-modified GCE (TYR/GA/GO/GCE)

Prior to the fabrication of the biosensor, the bare glassy carbon electrode (GCE, 3.0 mm in diameter) was mechanically polished successively on a micro-cloth with 1.0, 0.3, and 0.05 μm *α*-alumina slurries to obtain a mirror-like surface. The cleaned electrode was rinsed and sonicated with distilled water and ethanol to remove any adhering alumina. The as-obtained graphene oxide (GO) was dispersed in PBS (2.5 mg/mL) and exfoliated by ultrasonication for 1 h to obtain the yellow-brown dispersion. Unexfoliated GO was removed after 1 h of centrifugation.

Schematic 1 shows the preparation process of the TYR/GA/GO/GCE. First, 10 μL GO solution (2.5 mg/mL) was dropped onto the bare GCE (GO/GCE). Then, after 1 h of immobilization, the GO/GCE was washed under ultrasonication for 5 min and stirring for 5 min in pure water. After that, 10 μL of glutaraldehyde (GA) solution was cast onto the GO-modified GCE (GA/GO/GCE). After 15 min of immobilization, the GA/GO/GCE was washed under stirring three times, each time for 5 min. Finally, TYR concentrations ranging from 0 to 0.5 mg/mL (10 μL) were added to the GA/GO/GCE surface for 12 h. The as-obtained biosensor is denoted as TYR/GA/GO/GCE. The measurement principle of the present sensor is shown in Schematic 2. The cathodic current due to the reduction of *o*-quinones produced by TYR-catalyzed monophenolase and diphenolase activities was detected at -0.05 V vs. Ag/AgCl.

3. Results and Discussion

3.1 Characterization of the TYR/GA/GO/GCE

Biomolecule-functionalized support surfaces are of fundamental importance for substrate recognition in biosensor technology. The choice and selection of materials and their preparation are especially important in the development of electrochemical sensors. These days, graphene is the most popular material in physics[24] as the first example of a strictly two-dimensional (2-D) and one-atom-thick sheet, which has been attracting much attention due to its fascinating physical properties.[28,29] Recently, various graphene oxide composites have been analyzed for understanding the performance of the fabricated biosensor. The structures and functional groups of GO,

GA/GO and TYR/GA/GO were examined by FT-IR spectroscopy, which is presented in Fig. 1. The peaks at approximately $_{max}$/cm^{-1} 3200 cm^{-1} (O-H stretching), 1716 cm^{-1}, and 1635 cm^{-1} (C=O stretching) are attributed to the oxygen-containing functional groups on GO. The FT-IR data demonstrate good consistency with the previous paper.[30] Many bio-functional materials were applied with different degrees of success to develop a sensitive, stable and reusable support surface. In our case, the hydroxyl (-OH) group on the graphene oxide is useful for the covalent coupling of protein to the surface.

After GA modification on the GO support matrix, there is a sharp decrease of the peak range from $_{max}$/cm^{-1} 3000 to 3500 (Fig. 1b). We speculate this is due to the covalent bonding between the –OH group of GO and the C=O group of GA. Meanwhile, the peak at 1716 cm^{-1} increased, and its existence is evidence of the C=O group because of the overlay of GA onto the GO surface. Finally, the new peak appearing at $_{max}$/cm^{-1} 1559 proved the bonding between –NH_2 belonging to TYR and the C=O of GA (Figure 1c). This coincides with the assembly protocol as shown in Schematic 1.

Field emission scanning electron microscopy was used to evaluate the structure and morphology of the modified GCE as shown in Fig. 2. It can be seen that the GO-modified GCE exhibited a typical crumpled and wrinkled sheet structure of GO (Fig. 2B), which provides a hydroxyl (-OH)-containing surface for the further immobilization of enzymes. After GA immobilization, the GA/GO formed a homogeneous dotty film (Fig. 2C), indicating the successful immobilization of GA on the surface of the GO-modified GCE. Additionally, the snowflake-like morphology is evidence of TYR self-assembly (Fig. 2D). The successful immobilization was also proven by the cyclic voltammograms to check the catechol-detected response by using different immobilization procedures (Figure S1).

In addition, the AFM images with the height profiles of the GCE modified with GO (Fig. 3A), GA/GO (Fig. 3B) and TYR/GA/GO (Fig. 3C) were evaluated. The GO-modified GCE expressed a relative smooth surface. After GA modification, the surface showed a much shriller and rough morphology, probably due to

surface-attached GA. Then, after TYR modification, the surface smoothness was recovered. Contrary to the prediction, the height of the TYR/GA/GO (C) was not increased much (rather decreased) compared with the GA/GO (B). These observations suggest that enzymes with flexible conformations may change their conformation by covalent bonding with GA, by interfacial interaction with GO, and by lateral interaction between neighboring TYR molecules. Similar changes in the morphology and surface roughness after enzyme immobilization have been reported. [31]

3.2 Electrochemical studies of TYR/GA/GO/GCE

The electrocatalytic activity and electron transfer properties of the immobilized enzymes on the electrodes are significantly affected by the conformations and structures of the enzymes on the electrode surfaces. Therefore, to obtain the interfacial properties of modified electrodes, we measured cyclic voltammograms (CV) of 1 mM $[Fe(CN)_6]^{3-/4-}$ on the bare GCE (orange), GO/GCE (blue), GA/GO/GCE (green) and TYR/GA/GO/GCE (red) by using in 0.1 M PBS (pH = 7.0) at a scan rate of 100 mV/s (Figure 4A). The peak-to-peak separations are different among these four electrodes. These results would reflect the differences in the structure and morphology of the modified electrode surfaces.

The electrochemical behaviors of the modified electrodes were also investigated by EIS using $[Fe(CN)_6]^{3-/4-}$ as a redox probe. It is also one of the important parameters to evaluate the interfacial properties of protein-modified electrodes.[32] Figure 4B shows the Nyquist plots of the EIS for the bare GCE (orange triangle), GO/GCE (blue circle), GA/GO/GCE (green triangle), and TYR/GA/GO/GCE (red circle) obtained in 0.1 M phosphate buffer solution containing 1 mM $[Fe(CN)_6]^{3-/4-}$. The value of the electron transfer resistance (R_{ct}) could be obtained from the semicircle diameter, which equaled the R_{ct} and varied with the presence of different substances on the electrode surface. As shown, the R_{ct} of the GO/GCE (21 kΩ) is larger than that of the bare GCE (500 Ω), suggesting that a layer of GO film has formed on the surface of the GCE and hindered the charge transfer from the $[Fe(CN)_6]^{3-/4-}$ redox probe to the GCE surface. Obviously, the R_{ct} of the TYR/GA/GO/GCE is dramatically increased to 105 kΩ due to the blocking effects of TYR on charge transfer, which also indicates

that TYR has been successfully immobilized. This interpretation would also be supported by the results of the CVs of each electrode (Fig. 4A).

3.3 Electrochemical response characteristics of catechol on the TYR/GA/GO/GCE

Figure 5 shows the CVs of the TYR/GA/GO/GCE in deoxygenated 0.1 M PBS (pH = 7.0) containing catechol with different scan rates (ν). As proven in Fig. 5, the I_{pa} and I_{pc} of catechol increased with increasing scan rates from 0.01 to 0.1 V s^{-1}. As shown in Fig. 5 (inset), the I_{pa} and I_{pc} of catechol gradually increased in a good linear relationship with the square root of the scan rate ($\nu^{1/2}$) in the range of 0.01 to 0.1 V s^{-1}. This result strongly demonstrated that this electrochemical process on the TYR/GA/GO/GCE was a diffusion-controlled process.[33]

To investigate the bioelectrocatalytic behavior of the TYR/GA/GO/GCE, we measured cyclic voltammograms (CVs) in air-saturated 0.1 M PBS (pH = 7.0). Figure 6 compares the CVs for 0.1 mM phenol derivatives (*p*-CP, *p*-cresol, phenol and catechol) recorded at 5 mV/s. TYR has broad specificity toward various mono- and diphenolic compounds, and the substrate selectivity of TYR usually is according to the following trend: catechol ≫ *p*-cresol > *p*-CP > phenol.[34,35] Here, we used the sensitivity (the magnitude of the cathodic current of the CV) as an indication of the selectivity toward various phenolic compounds because the sensitivity reflects the bioelectrocatalytic activity of the present TYR/GA/GO/GCE-based biosensor, and we obtained the following trend in the sensitivity of the TYR-GCE-based biosensor: catechol > *p*-cresol > *p*-CP > phenol.

3.4 Optimization of the experimental variables

3.4.1 Effect of the GA concentration on the current response

The effect of the GA concentration on the steady-state cathodic current response to 10 μM catechol obtained at -0.05 V vs. Ag/AgCl in 0.1 M PBS (pH = 7.0) is shown in Figure 7 A. It can be seen that the current increased as the concentration of GA increased from 0 to 20% (V/V%) and then decreased when the GA concentration was increased to 25%. It could be assumed that a high concentration of toxic of GA is not preferable for the enzyme. In the absence of GA, no apparent response to catechol was observed, indicating that GA is essential for the covalent bonding of TYR in the

preparation of this biosensor. This is also in accordance with CVs by measuring different modified electrodes (GO/GCE, GA/GO/GCE and TYR/GA/GO/GCE) in air-saturated PBS solution at a scan rate of 100 mV/s (Figure S1). The background current of the GO/GCE (Fig. S1a) is larger than that of the GA/GO/GCE (Fig. S1b). It is ascribed to the improvement of the electrical conductivity where no electrochemical reaction is observed; curve b is a cyclic voltammogram of a GA/GO/GCE electrode with the experimental conditions as for a, where no peak also appears. Curve c is a cyclic voltammogram of a TYR/GA/GO/GCE electrode with the experimental conditions as for a, which possesses a sharp reductive peak at -0.04 V.

3.4.2 Effect of the pH of the electrolyte on the current response

The effect of the electrolyte pH on current response to catechol was investigated over the pH range from 5.0 to 8.5 using 0.1 M PBS (Figure 7 B), and the maximum current response was obtained at a pH of 7.0. This optimum pH range was in good accordance with the irreversible loss of activity below 4.5 and beyond 9.3 observed for the free TYR.[36] In addition, the optimized pH is similar with the reported TYR-based catechol sensor.[37] This indicates that the present immobilization procedure has not altered the activity of TYR. Therefore, 0.1 M pH = 7.0 PBS was chosen at the supporting electrolyte solution in this work.

3.4.3 Effect of the TYR concentration on the current response

The effect of the enzyme concentration on the current response to catechol was investigated. As shown in Fig. 7 C, the current increased with the increase of the concentration of TYR immobilized on the electrode up to 0.5 mg/mL. When the concentration was more than 0.5 mg/mL, the current decreased with the increase of the TYR concentration. If a higher concentration of the enzyme solution during the immobilization of TYR (immobilization time is 12 h) leads to three-dimensional enzyme deposition at the electrode surface, the phenomena can be attributed to a decrease in the recycling process and/or to steric hindrance toward the diffusion of the substrates and products of the enzymatic reaction.[38] Therefore, 0.5 mg/mL TYR was chosen for all subsequent experiments.

3.4.4 Effect of the applied potential on the response current

Figure 7 D shows the effect of the applied potential (between -0.15 and 0.1 V) on the response current to 10 μM catechol. Under the applied potential range, the response signal and background current were tested. The highest ratio of signal-to-background current was achieved at -0.05 V. When the applied potential was more negative than -0.1 V, the background current due to the electrochemical reduction of dissolved oxygen significantly increased, leading to a decrease of the ratio of the signal-to-background current. Therefore, -0.05 V was selected as the applied potential for further studies.

Furthermore, the effects of the GO concentration and TYR immobilization time were also optimized (Fig. S2 and Fig. S3). The best results were obtained with a GO concentration of 2.5 mg/mL and a TYR immobilization time of 12 hours, respectively. The efficiencies of various coupling reagents were also investigated by using six kinds of reagents, among which GA showed the best result (Fig. S4).

3.5 Linear range and detection limit

Figure 8 shows a typical current-time curve for the TYR/GA/GO/GCE biosensor upon successive additions of catechol to air-saturated PBS (pH = 7.0) under stirring with a working potential of -0.05 V. Upon the addition of successive aliquots of catechol to the buffer solution, a clearly defined reduction current proportional to the catechol concentration was observed, which is attributed to the reduction of *o*-quinone enzymatically formed. The sensor response achieves 95% of the steady-state-current in less than 3 seconds.

The TYR/GA/GO/GCE biosensor showed an extremely wide linear range for catechol from 5.0×10^{-8} to 5.0×10^{-5} M and the regression equation $I=0.3377c+0.0418$, with a correlation coefficient of 0.9981. The limit of detection (LOD) was as low as 3.0×10^{-8} M (S/N = 3).

Table 1 summarizes some characteristics of recently reported TYR-based phenol biosensors compared with our TYR/GA/GO/GCE biosensor. Some other sensors exhibit superior analytical performance (i.e., wider linear range, lower detection limit, and higher sensitivity). However, the considerable advantages of the present TYR/GA/GO/GCE biosensor would be the facile preparation protocol, fast response

time, low cost, and practical usage (described below).

3.6 Repeatability, reproducibility, long-term stability and interference

The repeatability and reproducibility of the TYR/GA/GO/GCE biosensor have been assessed. The fabricated biosensor showed good repeatability with a relative standard deviation (RSD) of 4.9% for 10 successive measurements of 10 μM catechol. To evaluate the intra-day precision (between lot-variation) of the present sensor, 5 sensors were prepared in the same manner on the same day, and the current response to 10 μM catechol was measured. The RSD value (n＝5) for the current response to catechol obtained by different sensors was 2.7%. These results indicate that the present sensor preparation protocol has acceptable reliability.

Furthermore, the biosensor has favorable storage stability. The fabricated biosensor was stored in 0.1 M PBS at 4°C, and the current response to catechol was checked every 5 days. Even after a month of storage, the sensor retained 77% of its initial current response. Therefore, it is safe to say that this biosensor has a storage stability within the range of the maximum stabilities already reported.[44]

To evaluate the selectivity of the biosensor, the influence of some possible interfering substances was checked in PBS (pH = 7.0). Table 2 summarizes the recoveries of 10 μM catechol in the presence of 100-fold concentrations (1 mM) of K^+, Cu^{2+}, Mg^{2+}, SO_4^{2-}, and PO_4^{3-} as well as 10-fold concentrations (0.1 mM) of glucose, AA, UA, and hydrogen peroxide. The results suggested that the TYR/GA/GO/GCE biosensor exhibits no significant interference in the presence of the tested ions and compounds.

3.7 Analytical applications

To study the real feasibility of the TYR/GA/GO/GCE biosensor, we checked the applicability of the biosensor in the determination of phenols in real water samples (obtained from our lab). No special sample pretreatment was required. The results are shown in Table 3. The RSD and recovery were less than 1.9% and 100.5-101.8% for the present biosensor, suggesting that the TYR/GA/GO/GCE biosensor can be used to detect and measure the concentration of phenol derivatives in real samples with reasonably good performance. The total assay time including sample preparation,

sample measurement and data processing is less than 1 h.

4. Conclusions

We describe an amperometric biosensor, which was fabricated based on TYR immobilized onto a GO film, for the determination of phenol derivatives. Under the optimum conditions, the TYR/GA/GO/GCE biosensor exhibited a wide sensing linear range from 5×10^{-8} M to 5×10^{-5} M, lower detection limit of 3×10^{-8} M, current maxima (I_{max}) of 65.8 μA and apparent Michaelis constant (K_m^{app}) of 169.9 μM for catechol. Compared with other TYR-based biosensors reported in the literature, the TYR/GA/GO/GCE biosensors reported in this work possess various advantages including a simple fabrication protocol, excellent performance in terms of the response rate, a wide linear range, a rapid response time, good operational stability and a long lifetime.

Conflicts of interest

There are no conflicts of interest to declare.

Acknowledgements

The authors gratefully acknowledge the financial support from the Natural Science Foundation of Liaoning Province (No. 20170540464), the Department of Education of Liaoning (No. 2017LNQN05) and the Foundation of University of Science and Technology, Liaoning (No. 2015QN08 and No. 2016RC12).

References

[1] S. Seo, V.K. Sharma, N. Sharma, Mushroom tyrosinase: recent prospects. J. Agric. Food Chem. 51 (2003) 2837-2853.

[2] G. Yong, C. Leone, K.G. Strothkamp, Agaricus bisporus metapotyrosinase: preparation, characterization, and conversion to mixed-metal derivatives of the binuclear site, Biochemistry 29 (1990) 9684-9690.

[3] W.T. Rajesh, K. Kaneto, Amperometric phenol biosensor based on covalent immobilization of tyrosinase onto an electrochemically prepared novel copolymer poly (*N*-3-aminopropyl pyrrole-co-pyrrole) film, Sens. Actuators B-Chem. 102 **(**2004) 271-277.

[4] N. Durán, E. Esposito, Potential applications of oxidative enzymes and phenoloxidase-like compounds in wastewater and soil treatment: a review, Appl. Catal. B: Environ. 28 **(**2000) 83-99.

[5] M. Castillo, R. Domingues, M.F. Alpendurada, D. Barceló, Persistence of selected pesticides and their phenolic transformation products in natural waters using off-line liquid solid extraction followed by liquid chromatographic techniques, Anal Chim Acta 353 (1997) 133-142.

[6] W.A. MacCrehan, J.M. Brown-Thomas, Determination of phenols in petroleum crude oils using liquid chromatography with electrochemical detection, Anal. Chem. 59 (1987) 477-479.

[7] T.A. Berger, J.F. Daye, Separation of phenols by packed column supercritical fluid chromatography, J Chromatogr Sci., 29 (1991) 54-59.

[8] L.B. Pérez, A. Merkoçi, Improvement of the electrochemical detection of catechol by the use of a carbon nanotube based biosensor, Analyst 134 (2009) 60-64.

[9] Y. Wang, Y. Hasebe, Acridine orange-induced signal enhancement effect of tyrosinase-immobilized carbon-felt-based flow biosensor for highly sensitive detection of monophenolic compounds, Anal. Bioanal. Chem. 399 (2011) 1151-1162.

[10] L.M. Kong, S.S. Huang, Z.L. Yue, B. Peng, M.Y. Li, J. Zhang, Sensitive mediator-free tyrosinase biosensor for the determination of 2,4-dichlorophenol, Microchim Acta 165 (2009) 203-209.

[11] Z.J. Liu, B.H. Liu, J.L. Kong, J.Q. Deng, Probing trace phenols based on mediator-free alumina sol-gel-derived tyrosinase biosensor, Anal. Chem. 72 (2000) 4707-4712.

[12] J.Z. Zhang, B.Q. Wang, B. Xu, G.J. Cheng, S.J. Dong, Amperometric quantification of polar organic solvents based on a tyrosinase biosensor, Anal. Chem. 72 (2000) 3455-3460.

[13] B. Serra, M.D. Morales, J.B. Zhang, A.J. Reviejo, E.H. Hall, J.M. Pingarron, In-a-day electrochemical detection of coliforms in drinking water using a tyrosinase composite biosensor, Anal. Chem. 22 (2005) 8115-8121.

[14] D.E. Goodney, T.P. Silverstein, Using the tyrosinase-based biosensor to determine the concentration of phenolics in wine, J. Chem. Educ. 90 (2013) 1710-1712.

[15] Y. Wang, Y. Hasebe, Carbon felt-based biocatalytic enzymatic flow-through detectors: Chemical modification of tyrosinase onto amino-functionalized carbon felt using various coupling reagents, Talanta 79 (2009) 1135-1141.

[16] W.R. Everett, G.A. Rechnitz, Mediated bioelectrocatalytic determination of organophosphorus pesticides with a tyrosinase-based oxygen biosensor, Anal. Chem. 70 (1998) 807-810.

[17] J. Wang, L. Chen, Hydrazine detection using a tyrosinase-based inhibition biosensor, Anal. Chem. 67 (1995) 3824-3827.

[18] D.E. Wilcox, A.G. Porras, Y.T. Hwang K. Lerch, M.E. Winkler, E.I. Solomon, Substrate analog binding to the coupled binuclear copper active site in tyrosinase, J. Am. Chem. Soc. 107 (1985) 4015-4027.

[19] E.I. Solomon, U.M. Sundaram, T.E. Machonkin, Multicopper oxidases and oxygenases, Chem. Rev. 96 (1996) 2563-2606.

[20] M.S. Fernandes, S. Kerkar, Microorganisms as a source of tyrosinase inhibitors: a review, Ann. Microbiol. 67 (2017) 343-358.

[21] S.C. Atlow, L. Bonadonna-Aparo, A.M. Klibanov, Dephenolization of industrial wastewaters catalyzed by polyphenol oxidase, Biotech. Bioeng. 26 (1984) 599-603.

[22] Y. Wang, Y. Hasebe, Tyrosinase-modified carbon felt-based flow-biosensors:

The role of ultra-sonication in shortening the enzyme immobilization time and improving the sensitivity for p-chlorophenol, J. Environ. Sci. 23 (2011) 1038-1043.

[23] K.S. Novoselov, A.K. Geim, S.V. Morozov, D. Jiang, Y. Zhang, S.V. Dubonos, I.V. Grigorieva, A.A. Firsov, Electric field effect in atomically thin carbon films, Science 306 (2004) 666-669.

[24] C.J. Zhao, X. Wu, P.W. Li, C.H. Zhao, X.Z. Qian, Hydrothermal deposition of CuO/rGO/Cu_2O nanocomposite on copper foil for sensitive nonenzymatic voltammetric determination of glucose and hydrogen peroxide, Microchim Acta 184 (2017) 2341-2348.

[25] Y. Zhu, S. Murali, W. Cai, X. Li, J.W. Suk, J.R. Potts, R.S. Ruoff, Graphene and Graphene Oxide: Synthesis, Properties, Adv. Mater. 22 (2010) 3906-3924.

[26] D.R. Dreyer, S. Park, C.W. Bielawski, R.S. Ruoff, The chemistry of graphene oxide, Chem. Soc. Rev. 39 (2010) 228-240.

[27] T. Kuila, S. Bose, P. Khanra, A.K. Mishra, N.H. Kim, J.H. Lee, Recent advances in graphene-based biosensors, Biosens. Bioelectron. 26 (2011) 4637-4648.

[28] C. Lee, X. Wei, J.W. Kysar, J. Hone, Measurement of the elastic properties and intrinsic strength of monolayer graphene, Science 321 (2008) 385-388.

[29] A.K. Geim, K.S. Novoselov, The rise of graphene, Nat. Mater. 6 (2007) 183-191.

[30] J. Chen, Y.L. Jin, Sensitive phenol determination based on co-modifying tyrosinase and palygorskite on glassy carbon electrode, Microchim Acta 169 (2010) 249-254.

[31] V. Sethuraman, P. Muthuraja, J. Anandha Raj, P. Manisankar, A highly sensitive electrochemical biosensor for catechol using conducting polymer reduced graphene oxide–metal oxide enzyme modified electrode, Biosens. Bioelectron. 84 (2016) 112-119.

[32] Q. Chi, J. Zhang, J.U. Nielsen, E.P. Friis, I. Chorkendorff, G.W. Canters, J.E.T. Andersen, J. Ulstrup, Molecular monolayers and interfacial electron transfer of pseudomonas aeruginosa azurin on Au(111), J. Am. Chem. Soc. 122 (2000) 4047-4055.

[33] D.J. Rao, X.J. Zhang, Q.L. Sheng, J.B. Zheng, Highly improved sensing of

dopamine by using glassy carbon electrode modified with MnO_2, graphene oxide, carbon nanotubes and gold nanoparticles, Microchim Acta 183 (2016) 2597-2604.

[34] M.W.J. Ducey, M.E. Meyerhoff, Microporous gold electrodes as combined biosensor/electrochemical detectors in flowing streams, Electroanalysis 10 (1998) 157-162.

[35] G. Marko-Varga, E. Burestedt, C.J. Svensson, J. Emneus, T. Ruzgas, M. Lutz, K.K. Unger, Effect of HY-zeolites on the performance of tyrosinase-modified carbon paste electrodes, Electroanalysis 8 (1996) 1121-1126.

[36] D. Kertesz, R. Zito, Mushroom polyphenol oxidase I. Purification and general properties, Biochimica et Biophysica Acta (BBA) - Nucleic Acids and Protein Synthesis, Biochim. Biophy. Acta 96 **(**1965) 447-462.

[37] Y.S. Zou, D. Lou, K. Dou, L.L. He, Y.H. Dong, S.L. Wang, Amperometric tyrosinase biosensor based on boron-doped nanocrystalline diamond film electrode for the detection of phenolic compounds, J Solid State Electrochem 20 (2016) 47-54.

[38] S. Cosnier, I.C. Popescu, Poly(amphiphilic pyrrole)-tyrosinase-peroxidase electrode for amplified flow injection-amperometric detection of phenol, Anal Chim Acta 319 (1996) 145-151.

[39] S.F. Rahman, K. Min, S.H. Park, J.H. Park, J.C. Yoo, D.H. Park, Highly sensitive and selective dopamine detection by an amperometric biosensor based on tyrosinase/MWNT/GCE, Korean J. Chem. Eng. 33 (2016) 3442-3447.

[40] H.Q. Li, X. Hu, H.M. Zhu, Y. Zang, H.G. Xue, Amperometric phenol biosensor based on a new immobilization matrix: polypyrrole nanotubes derived from methyl orange as dopant, Int. J. Electrochem. Sci. 12 (2017) 6714-6728.

[41] F.C. Vicentini, L.L.C. Garcia, L.C.S. Figueiredo-Filho, B.C. Janegitz, O. Fatibello-Filho, A biosensor based on gold nanoparticles, dihexadecylphosphate, and tyrosinase for the determination of catechol in natural water, Enzyme and Microbial Technology 84 (2016) 17-23.

[42] E. Araque, R. Villalonga, M. Gamella, P. Martínez-Ruiz, J. Reviejo, J.M. Pingarrón, Crumpled reduced graphene oxide–polyamidoamine dendrimer hybrid nanoparticles for the preparation of an electrochemical biosensor, J. Mater. Chem. B 1

(2013) 2289-2296.

[43] B. Borisova, J. Ramos, P. Díez, A. Sánchez, C. Parrado, E. Araque, R. Villalonga, J.M. Pingarrón, A Layer-by-Layer biosensing architecture based on polyamidoamine dendrimer and carboxymethylcellulose-modified graphene oxide, Electroanalysis 27 (2015) 2131-2138.

[44] S. Cosnier, J.J. Fombon, P. Labbé, D. Limosin, Development of a PPO-poly(amphiphilic pyrrole) electrode for on site monitoring of phenol in aqueous effluents, Sens. Actuators B 59 (1999) 134-139.

Table 1 Summary of the TYR-based catechol biosensors reported in the literature

Sensors	Linear range (μM)	LOD (μM)	Sensitivity (μA/μM)	Ref
TYR/BDND/film electrode	5-120	2.35	0.096	37
TYR/MWNT/GCE	50-1000	50	1.323	39
PPy-NTs/PPO	0.1-35	0.0012	2.981	40
PEDOT-rGO-Fe_2O_3-PPO	0.04-62	0.007	------	31
TYR-AuNPs-DHP/GCE	2.5-95	0.17	0.115	41
TYR-PAMAM-Sil-rGO/GCE	0.01-22	0.006	0.424	42
TYR/PAMAM/GO-CMC/GCE	0.002-0.4	0.0009	6.3	43
TYR/GO/GA/GCE	0.05-50	0.03	0.34	This work

TYR, tyrosinase; BDND, boron-doped nanocrystalline diamond; MWNT, multiwalled nanotubes; GCE, glassy carbon electrode; GA, glutaraldehyde. PPy-NTs, polypyrrole nanotubes; PPO, polyphenol oxidase; PEDOT, poly(3,4-ethylenedioxythiophene); rGO, reduced graphene oxide; AuNPs, gold nanoparticles; DHP, dihexadecylphosphate; PAMAM, polyamidoamine dendrimer; Sil-rGO, silanized rGO; CMC, carboxymethyl cellulose.

Table 2 Recovery (%) obtained for 10 μM catechol in the presence of different interferents

Interferents	Ca^{2+}	Mg^{2+}	Cu^{2+}	PO_4^{3-}	SO_4^{2-}	glucose	AA	UA	H_2O_2
Recovery (%)	104.3	95.4	109.5	91.9	97.7	96.7	96.3	104.9	103.5

Table 3 Recovery of the TYR/GA/GO/GCE biosensor for the determination of real samples (n = 3)

Sample	Found (M)	Catechol added (μM)	Found (μM)	RSD[a] (%)	Recovery (%)
1	Not found	50	50.9	1.9	101.8
2	Not found	100	101.6	1.5	101.6
3	Not found	200	200.9	1.1	100.5

[a] RSD (%) calculated from three separate experiments.

Schematic 1

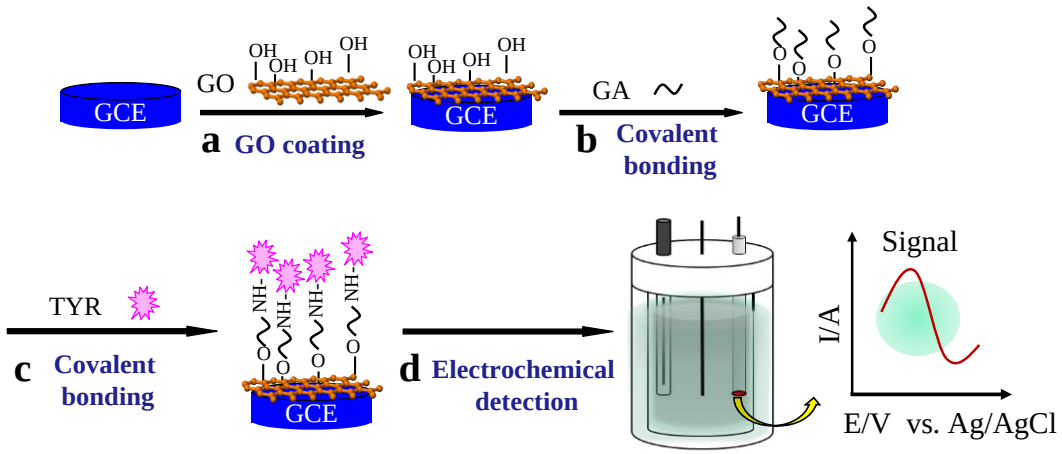

Schematic 1 Schematic illustration of the TYR/GA/GO/GCE biosensor for the electrochemical determination of phenol derivatives: *a*, GO coating; *b*, covalent bonding of GO and GA; *c*, covalent bonding of GA and TYR; and *d*, electrochemical detection of phenol derivatives.

Schematic 2

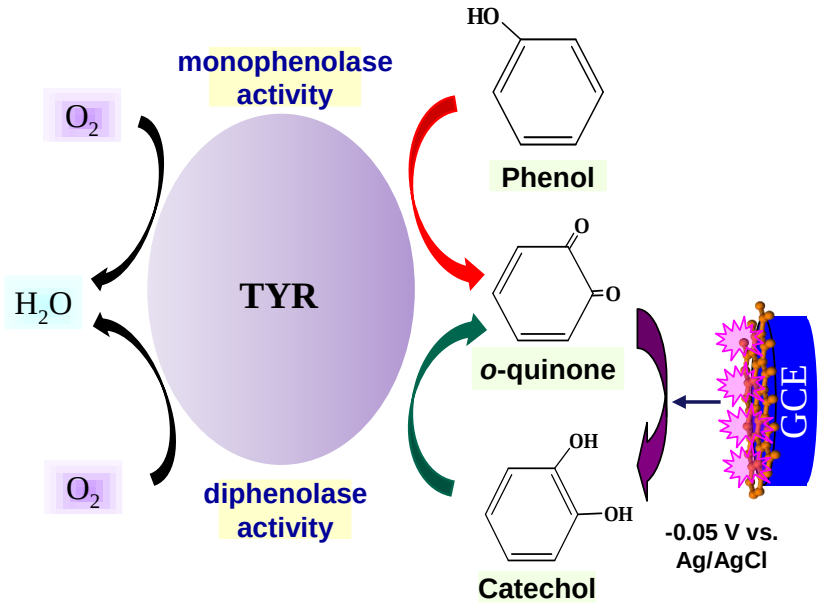

Schematic 2 Measurement principle of the present TYR/GA/GO/GCE biosensor.

Figure 1

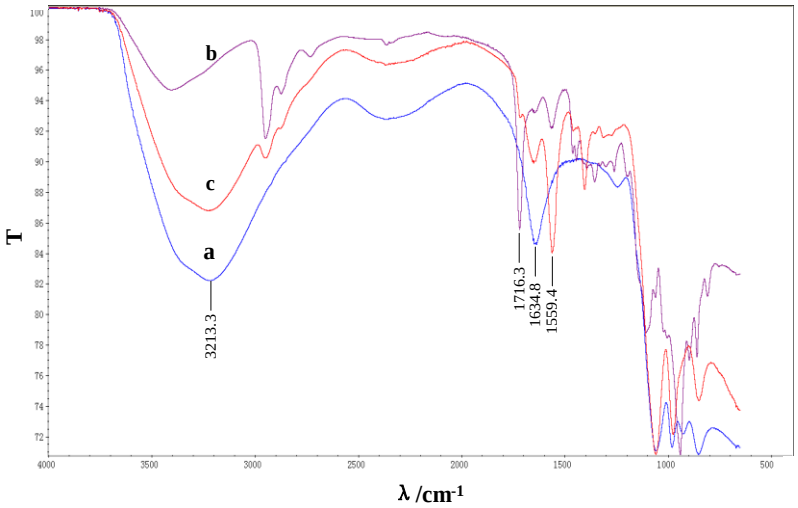

Figure 1 FT-IR spectra of GO (a), GA/GO (b) and TYR/GA/GO (c).

Figure 2

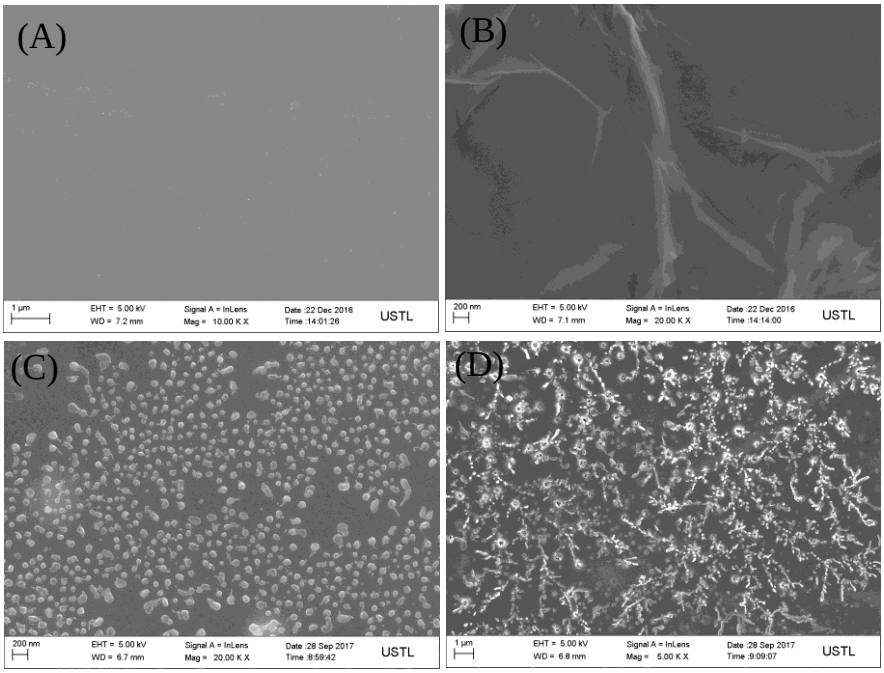

Figure 2 FE-SEM images of the (A) bare GCE, (B) GO/GCE, (C) GA/GO/GCE, and (D) TYR/GA/GO/GCE.

Figure 3

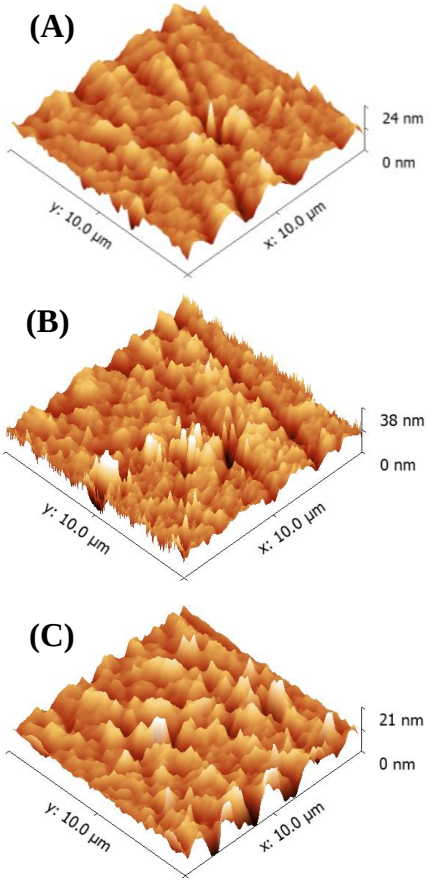

Figure 3 AFM images of GCEs modified with GO (A), GA/GO (B), and TYR/GA/GO (C) as well as their height profiles.

Figure 4

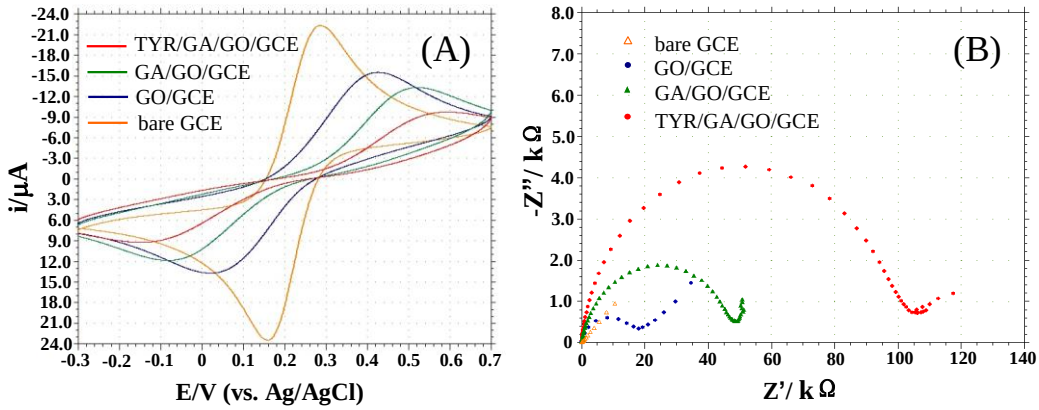

Figure 4 (A) CV behavior of the modified GCE in the presence of 1 mM $[Fe(CN)_6]^{4-/3-}$ in a deoxygenated 0.1 M PBS (pH = 7.0) at a scan rate of 100 mV s^{-1}. The starting potential is 0.7 V vs. Ag/AgCl. (B) EIS behavior of the modified GCE measured in the presence of 1 mM $[Fe(CN)_6]^{4-/3-}$ in a deoxygenated 0.1 M PBS (pH = 7.0). Bare GCE (orange), GO/GCE (blue), GA/GO/GCE (green), and TYR/GA/GO/GCE (red).

Figure 5

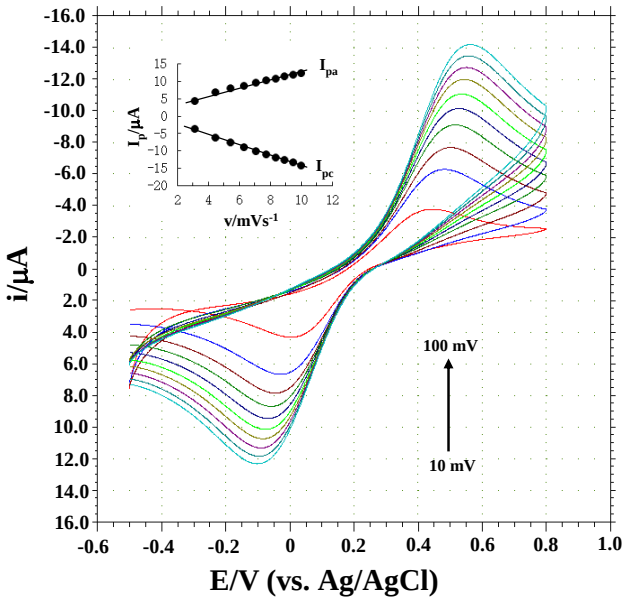

Figure 5 CVs obtained by the TYR/GA/GO/GCE in deoxygenated 0.1 M PBS (pH = 7.0) containing 1.0 mM catechol with different scan rates (from inner to outer: 0.01, 0.02, 0.03, 0.04, 0.05, 0.06, 0.07, 0.08, 0.09 and 0.1 V s^{-1}). Inset: linear fitting chart of the I_{pa} and I_{pc} of catechol versus $v^{1/2}$. The starting potential is 0.8 V vs. Ag/AgCl.

Figure 6

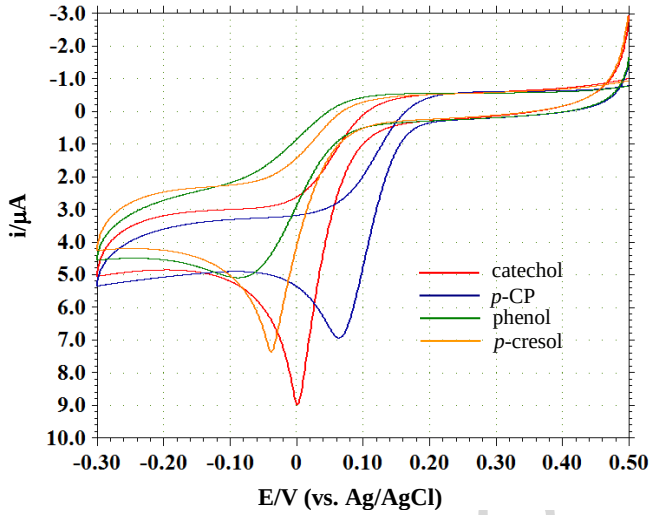

Figure 6 Cyclic voltammograms (CVs) in air-saturated 0.1 M PBS (pH = 7.0) containing 0.1 mM phenol derivatives (catechol, *p*-CP, phenol and *p*-cresol). The potential scan rate is 5 mV/s. The starting potential is +0.5 V vs. Ag/AgCl.

Figure 7

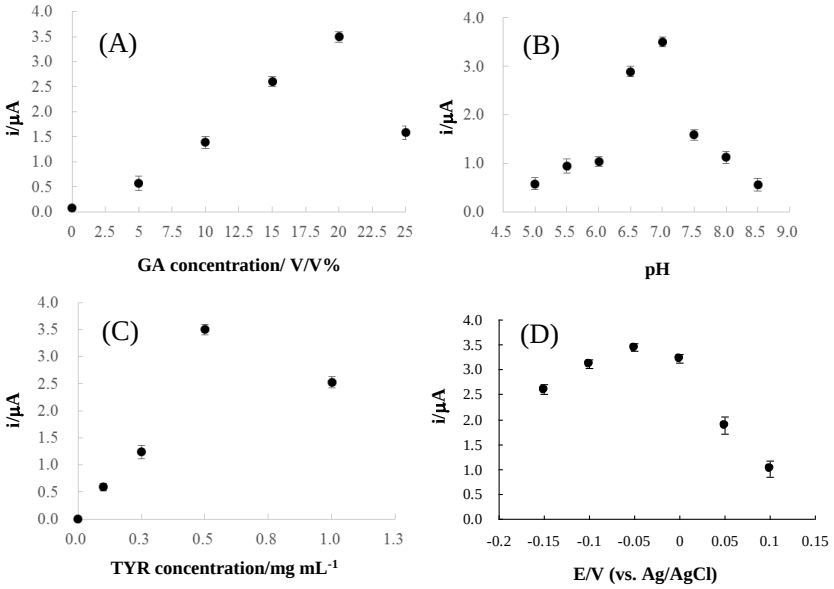

Figure 7 (A) Effect of the GA concentration on the amperometric response to 10 μM catechol in air-saturated 0.1 M PBS (pH = 7.0). (B) Effect of the pH on the amperometric response to 10 μM catechol. (C) Effect of the TYR concentration on the amperometric response to 10 μM catechol. (D) Effect of the applied potential on the amperometric response to 10 μM catechol. The applied potential is -0.05 V vs. Ag/AgCl for (A) to (C).

Figure 8

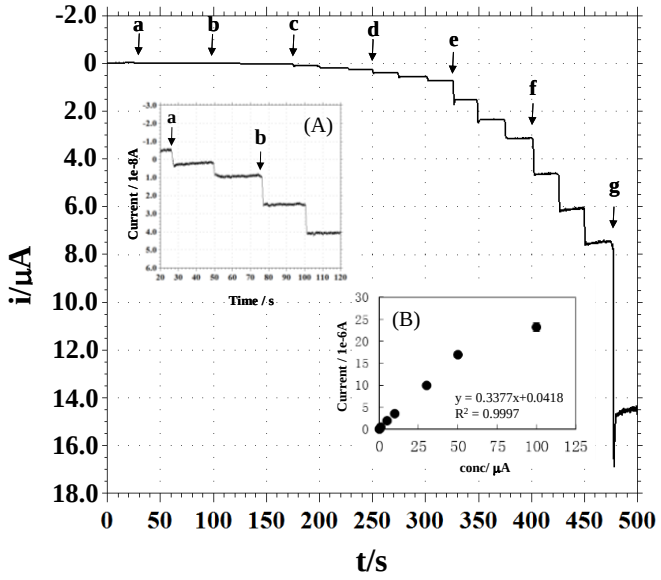

Figure 8 Amperometric current-time response curve of catechol obtained by the TYR/GA/GO/GCE biosensor (a: 50 nM; b: 0.1 μM; c: 0.5 μM; d: 1 μM; e: 5 μM; f: 10 μM; and g: 50 μM). Inset (A): Enlargement of the response curve at the lower concentration region. (B) Calibration curve for catechol concentrations from 5×10^{-8} M to 1×10^{-4} M. The applied potential is -0.05 V vs. Ag/AgCl.

Figure captions

Schematic 1 Schematic illustration of the TYR/GA/GO/GCE biosensor for the electrochemical determination of phenol derivatives: *a*, GO casting; *b*, covalent bonding of GO and GA; *c*, covalent bonding of GA and TYR; and *d*, electrochemical detection of phenol derivatives.

Schematic 2 Measurement principle of the present TYR/GA/GO/GCE biosensor.

Figure 1 FT-IR spectra of GO (a), GA/GO (b) and TYR/GA/GO (c).

Figure 2 FE-SEM images of the (A) bare GCE, (B) GO/GCE, (C) GA/GO/GCE, and (D) TYR/GA/GO/GCE.

Figure 3 AFM images of GC electrodes modified with GO (A), GA/GO (B), and TYR/GA/GO (C) as well as their height profiles.

Figure 4 (A) CV behavior of the modified GCE in the presence of 1 mM $[Fe(CN)_6]^{4-/3-}$ in deoxygenated 0.1 M PBS (pH = 7.0) at a scan rate of 100 mV s^{-1}. The starting potential is 0.7 V vs. Ag/AgCl. (B) EIS behavior of the modified GCE measured in the presence of 1 mM $[Fe(CN)_6]^{4-/3-}$ in a deoxygenated 0.1 M PBS (pH = 7.0). Bare GCE (orange), GO/GCE (blue), GA/GO/GCE (green), and TYR/GA/GO/GCE (red).

Figure 5 CVs obtained by the TYR/GA/GO/GCE in deoxygenated 0.1 M PBS (pH = 7.0) containing 1.0 mM catechol with different scan rates (from inner to outer: 0.01, 0.02, 0.03, 0.04, 0.05, 0.06, 0.07, 0.08, 0.09 and 0.1 V s^{-1}). Inset: linear fitting chart of the I_{pa} and I_{pc} of catechol versus $v^{1/2}$. The starting potential is 0.8 V vs. Ag/AgCl.

Figure 6 Cyclic voltammograms (CVs) in air-saturated 0.1 M PBS (pH = 7.0) containing 0.1 mM phenol derivatives (catechol, *p*-CP, phenol and *p*-cresol). The potential scan rate is 5 mV/s. The starting potential is +0.5 V vs. Ag/AgCl.

Figure 7 (A) Effect of the GA concentration on the amperometric response to 10 μM catechol in air-saturated 0.1 M PBS (pH = 7.0). (B) Effect of the pH on the amperometric response to 10 μM catechol. (C) Effect of the TYR concentration on the amperometric response to 10 μM catechol. (D) Effect of the applied potential on the amperometric response to 10 μM catechol. The applied potential is -0.05 V vs. Ag/AgCl for (A) to (C).

Figure 8 Amperometric current-time response curves of catechol obtained by the TYR/GA/GO/GCE biosensor (a: 50 nM; b: 0.1 μM; c: 0.5 μM; d: 1 μM; e: 5 μM; f: 10 μM; and g: 50 μM). Inset (A): Enlargement of the response curve at the lower concentration region. (B) Calibration curve for catechol concentrations from 5×10^{-8} M to 1×10^{-4} M. The applied potential is -0.05 V vs. Ag/AgCl.

Graphical abstract

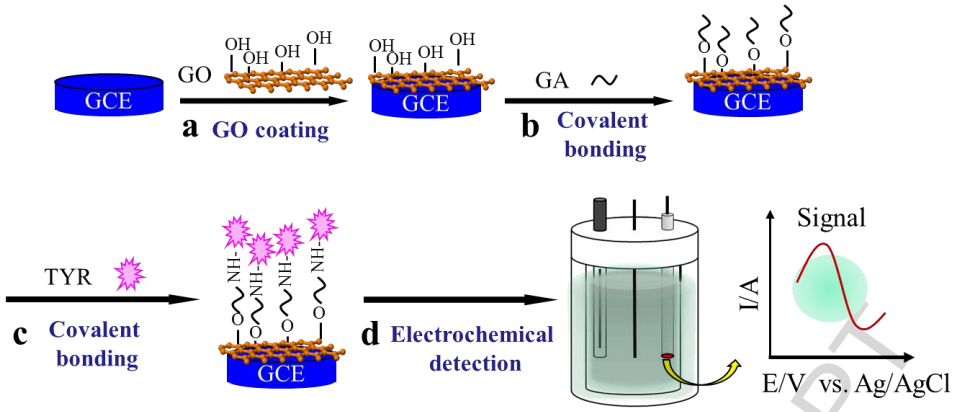

Schematic illustration of the TYR/GA/GO/GCE biosensor for electrochemical determination of phenol derivatives

Highlights

- Covalent bonding instead of adsorption between graphene oxide and tyrosinase was used.
- The OH group was utilized for covalent bonding.
- The fabrication conditions were investigated and optimized.
- The method provides a wider choice for constructing phenol biosensors.